Journal of Physics D: Applied Physics

PAPER

Absorptive coding metasurface for further radar cross section reduction

To cite this article: Sai Sui *et al* 2018 *J. Phys. D: Appl. Phys.* **51** 065603

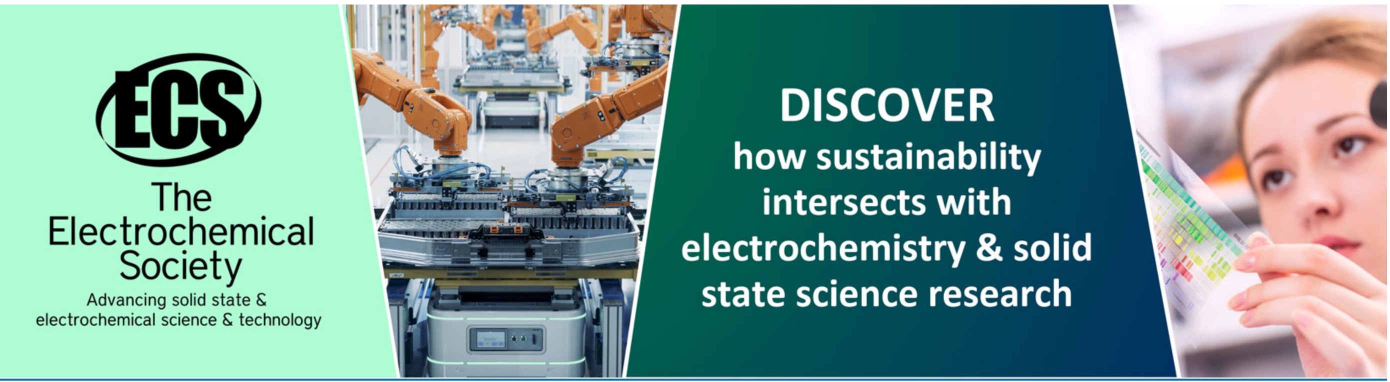

IOP Publishing Journal of Physics D: Applied Physics

J. Phys. D: Appl. Phys. **51** (2018) 065603 (6pp) https://doi.org/10.1088/1361-6463/aaa3be

Absorptive coding metasurface for further radar cross section reduction

Sai Sui[1], Hua Ma[1], Jiafu Wang[1], Yongqiang Pang[1,2], Mingde Feng[1], Zhuo Xu[2] and Shaobo Qu[1]

[1] College of Science, Air Force Engineering University, Xi'an, Shaanxi 710051, People's Republic of China

[2] School of Electronics and Information Engineering, Xi'an Jiaotong University, Xi'an, Shaanxi 710049, People's Republic of China

E-mail: mahuar@163.com

Received 27 September 2017, revised 8 December 2017
Accepted for publication 22 December 2017
Published 23 January 2018

Abstract

Lossless coding metasurfaces and metamaterial absorbers have been widely used for radar cross section (RCS) reduction and stealth applications, which merely depend on redirecting electromagnetic wave energy into various oblique angles or absorbing electromagnetic energy, respectively. Here, an absorptive coding metasurface capable of both the flexible manipulation of backward scattering and further wideband bistatic RCS reduction is proposed. The original idea is carried out by utilizing absorptive elements, such as metamaterial absorbers, to establish a coding metasurface. We establish an analytical connection between an arbitrary absorptive coding metasurface arrangement of both the amplitude and phase and its far-field pattern. Then, as an example, an absorptive coding metasurface is demonstrated as a nonperiodic metamaterial absorber, which indicates an expected better performance of RCS reduction than the traditional lossless coding metasurface and periodic metamaterial-absorber. Both theoretical analysis and full-wave simulation results show good accordance with the experiment.

Keywords: metamaterial, metasurface, coding metasurface, RCS

S Supplementary material for this article is available online

(Some figures may appear in colour only in the online journal)

Introduction

Over the past few decades, research on metamaterial has attracted much attention on microwave, terahertz and optical frequencies. Metamaterial has inspired many novel applications such as the stealth cloak, gradient index lenses, perfect absorber, polarization manipulation and many other devices; however, these have usually suffered from the obstacle of bulky thickness and loss [1]. The phase gradient metasurface, a typical two-dimensional metamaterial constituted of inhomogeneous arrays of a subwavelength resonator, provides a promising candidate. The characterized properties of electromagnetic waves, such as the polarization state, propagation direction and amplitude, can be manipulated by employing the anisotropic metasurface [1–4]. As well as focusing on the metasurface that controls the near and far-field scattering pattern based on different mechanisms, in particular, far-field pattern shaping such as diffusion and low radar cross section (RCS) has been significantly attractive because of the demand of stealth.

There are two strategies for reducing RCS: the first one is the usage of an absorber. Energy absorption of electromagnetic waves can be achieved by conventional and metamaterial absorbers, thus low RCS can be obtained. The perfect metamaterial absorber (PMA) was first proposed by Landy *et al* in 2008 [5] and many researchers made great efforts in achieving wideband and polarization insensitive PMA [6–11]. The second strategy for RCS reduction is the technology of controlling the reflection phase proposed by Paquay *et al* in 2007 [12]. The basic idea is tantamount to exploiting the cancellation effects arising from the well-known $180 \pm 37°$ phase-difference between the corresponding reflection coefficients [12–14]. However, the PMA can achieve nearly 100% absorption within a narrow band; in addition, the $180 \pm 37°$ phase-difference demand can be achieved in a limited band.

More recently, the concepts of coding, digital, and programmable metasurfaces have been introduced and experimentally demonstrated [15]. The coding metasurface (CM) concept brings out the connection between metasurface and information technology, which can achieve a more flexible manipulation of the far-field scattering pattern. Instead of using traditional full-wave simulation or the effective parameters to describe metasurfaces, the '0' and '1' element with opposite phase responses can be used to characterize the metasurface and quickly predict the far-field pattern. The manipulation of electromagnetic waves using CM has been widely investigated both at the frequency of microwaves and terahertz. One of the significant applications of CM is RCS reduction, based on the far-field pattern diffusion. However, so far, the proposed CMs are used by lossless coding elements [16–20].

In this paper, the absorptive coding metasurface (ACM) is proposed to achieve the functions of both shaping the far-field scattering pattern and absorption. A new strategy is adopted for realizing bistatic RCS reduction by redirecting electromagnetic energy to more directions through optimizing reflection arrangement and absorption. The general law of the ratio of '0' and '1' element and coding sequence is theoretically analyzed and implemented. As a verification, an ACM of low bistatic RCS is proposed.

Methods

We start by analyzing a CM with an absorptive element. We consider a CM under normal incidence of a plane wave as shown in figure 1, which consists of a two-dimensional array of $M \times N$ lattices, and the lattices are uniformly spaced with d.

The concept of RCS reduction can be explained by the principle of planar array theory [21]. For this ground plane, the array factor can be represented by

$$\mathrm{AF}(\theta,\varphi)=\sum_{m=1}^{M}\sum_{n=1}^{N}\mathrm{e}^{[\mathrm{j}(m-1)(kd\sin\theta\cos\varphi)+\mathrm{j}(n-1)(kd\sin\theta\sin\varphi)+\mathrm{j}\phi(m,n)]} \tag{1}$$

where $\phi(m,n)$ is the initial phase of the lattice, θ and φ are the elevation and azimuth angles for an arbitrary scattering direction respectively. Therefore, the general expression for the RCS of a scattering surface can be represented by

$$\sigma=10\log\left[\lim_{r\to\infty}\left(4\pi r^2\frac{|E_\mathrm{s}|^2}{|E_\mathrm{i}|^2}\right)\right] \tag{2}$$

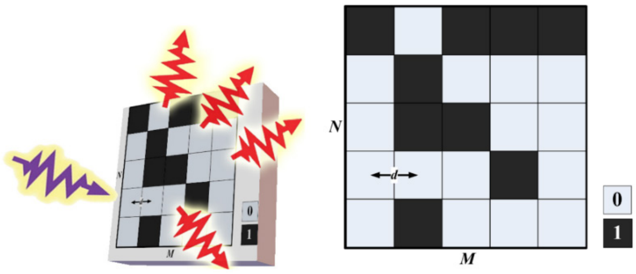

Figure 1. The ACM consisting of $M \times N$ lattices.

where $|E_\mathrm{s}|$ and $|E_\mathrm{i}|$ are the amplitudes of scattered and incident electric fields in the far zone of $r \to \infty$. For 1-bit CM, the basic element '0' and '1' can be characterized by A_0 and A_1 of the reflection coefficient amplitudes, as well as P_0 and P_1 of the reflection phase, respectively. Thus, the RCS reduction σ_r of 1-bit CM can be approximated through equation (3), in which the amplitude of the incident field is assumed as one.

$$\sigma_\mathrm{r}=10\log\left[\frac{A_0\mathrm{e}^{\mathrm{j}P_0}+A_1\mathrm{e}^{\mathrm{j}P_1}}{2}\right]^2. \tag{3}$$

In general, by introducing the ratio of coding element '0' and '1' into ACM, the ratio α is defined as $\alpha = n_0/n_1$, in which n_0 and n_1 are the number of '0' and '1' elements, respectively. Therefore, the RCS reduction in the normal incidence of 1-bit ACM can be expressed as equation (4).

$$\sigma_\mathrm{r}=10\log\left[\frac{\alpha A_0\mathrm{e}^{\mathrm{j}P_0}+A_1\mathrm{e}^{\mathrm{j}P_1}}{2}\right]^2. \tag{4}$$

Depending on equation (4), once the coding element of '0' and '1' are selected, this means the scattering amplitude and phase are determined. Once combined with a definite ratio, the RCS reduction of ACM in normal incidence is fixed. In other words, various coding sequences of fixed ratio have no influence on the RCS reduction of ACM in normal incidence. In addition to this, the ratio, scattered amplitude, and phase play the decisive role in RCS reduction. As shown clearly in figure 2, it is demonstrated how the phase difference of $P_\mathrm{d} = P_1 - P_0$ and ratio impact on RCS reduction. In figure 2(a), when the ratio of $\alpha = 1$, the ACM can be simplified as chessboard CM (there is an equal number of '0' and '1' elements as $n_0 = n_1$) and the 10 dB RCS reduction can be achieved in the well-known phase difference range of $180 \pm 37°$. In addition, from figure 2, with the corresponding absorption increase of '1' element from 0% to 90%, as $A_1 = 1$ changes to $A_1 = 0.1$, we conclude that the 10 dB RCS reduction demand of the phase difference becomes more and more relaxed in accordance with various ratios. Particularly, in figure 2(d), the $A_1 = 0.1$ means 90% absorption in accordance with $\alpha \to 0$, thus the ACM is simplified as a whole metamaterial absorber with 90% absorption.

Once the RCS reduction in normal incidence is determined, to achieve a wide-angle bistatic RCS reduction, the synthesis of an array pattern and genetic algorithm is

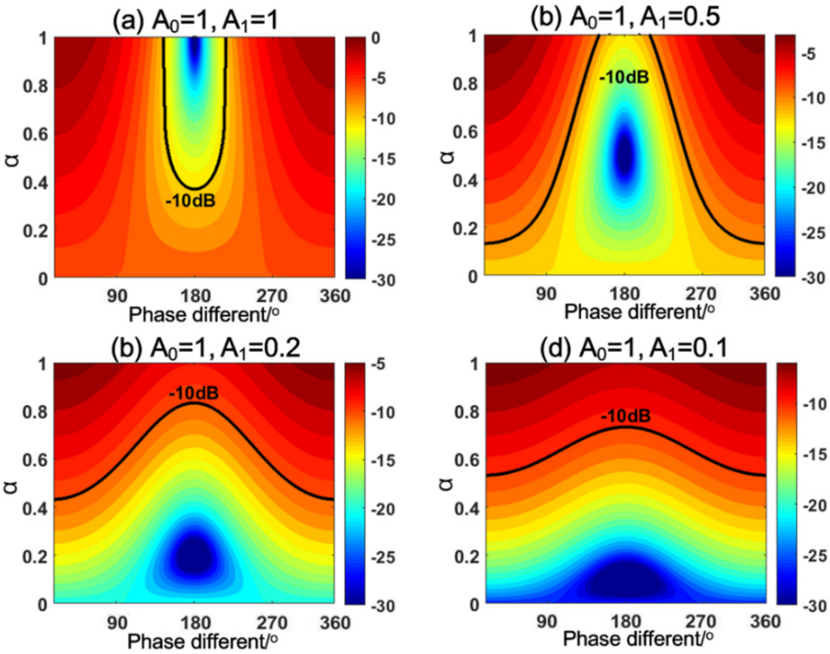

Figure 2. The RCS reduction in normal incidence with various phase differences and ratios. The scattering amplitude of '0' and '1' element are (a) $A_0 = 1, A_1 = 1$, (b) $A_0 = 1, A_1 = 0.5$, (c) $A_0 = 1, A_1 = 0.2$, (d) $A_0 = 1, A_1 = 0.1$, respectively.

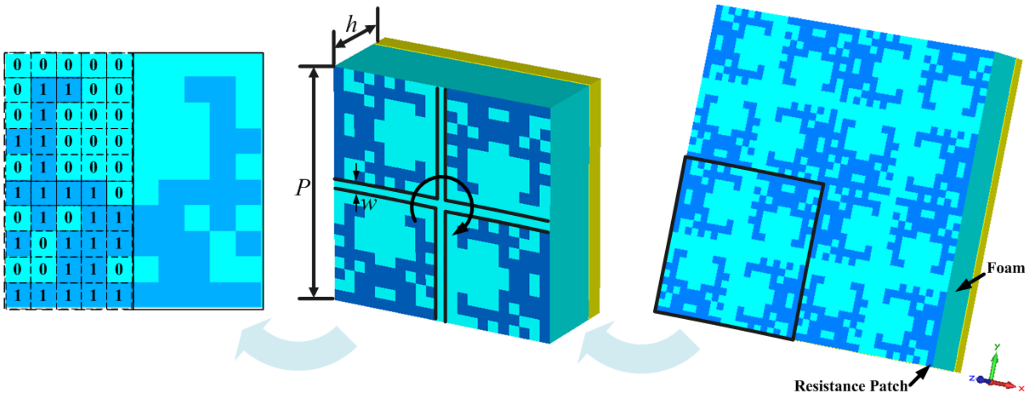

Figure 3. The configuration of coding element '1'.

employed. According to the theory of CM, the proper coding sequence can achieve far-field pattern shaping, which means reflective energy re-distribution in the desired direction. To get the best performance from the metasurface, the genetic algorithm is adopted together with a planar array pattern to obtain the optimal coding sequence. Firstly, the initial population with random coding sequence is established. Then, the fitness value of the initial population is calculated under the frame of fitness function. Next, the selection, crossover, and mutation operation are utilized until the runtime limitation is reached or iteration termination criterion is met. To evaluate the individual fitness, combining the array pattern factor, the fitness function is defined as

$$\text{fitness} = \max[\mathrm{AF}(\theta, \varphi)] \tag{5}$$

where the smaller the fitness value, the more homogeneous the distribution of the scattering field. When the optimization procedure is terminated, small fitness can be obtained, which means the optimal RCS reduction in abnormal incidence can be achieved.

Results

Based on previous analysis, we have established the simulation models of the coding elements of '0' and '1', which are characterized as the lossless element of π-phase-shifting and the absorptive element of zero-phase-shifting respectively. A PEC ground planar is selected as the '0' element without absorption. A wideband resistance frequency selective surface (RFSS) absorber is selected, combining topology optimization design, as the '1' element [22]. According to previous work, the topology design of a lightweight wideband polarization-independent RFSS absorber is selected. The absorption over a wide frequency range of 6.7–20 GHz with 90% absorption can be achieved by optimizing the topology and dimensions of the RFSS by the virtue of the genetic algorithm. The RFSS

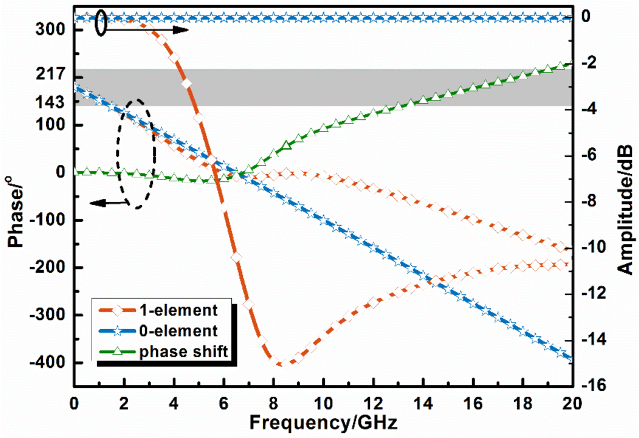

Figure 4. The simulation results of phase and amplitude of '0' and '1' coding element.

is then mounted on a grounded low-loss foam board with a relative permittivity of 1.1, as shown in figure 3. The surface resistance of carbon films is equal to $40\,\Omega\,\square^{-1}$, and the dimensional parameters are $p = 11.25$ mm, $w = 0.6$ mm, and $h = 3.6$ mm. Besides, the coding element of '0' is simplified as metallic ground, of which the dimensional parameters are equal to the coding element of '1'.

Both simulation results of '0' and '1' coding element are demonstrated in figure 4; as is shown clearly, the '1' element has 90% absorption in the range of 6.7–20 GHz, while '0' element has no absorption.

For further investigation, the theoretical prediction of the far-field pattern obtained by array pattern synthesis is demonstrated in figure 5 (available online at (stacks.iop.org/JPhysD/51/065603/mmedia)). From figures 5(a) and (b), we can see that the coding metasurface with lossless elements can achieve flexible control of the scattering pattern. As is shown clearly in figures 5(a) and (c), the absorber significantly decreases the value of RCS. In addition, the ACM, as shown in figure 5(d), achieves an inspiring performance for both RCS reduction and scattering manipulation. As a verification, the 3D pattern of bistatic RCS is obtained by full-wave simulation software in figure 6. For comparison, identical simulations are conducted with a PEC and absorber of equivalent geometry to that of the ACM in wideband range, as shown in figure 7. A wideband 10 dB reduction of RCS can be achieved in ACM over the frequency range of 6.5–20 GHz. In addition, the RCS of ACM obtains a reduction of more than 1.5 dB than that of the absorber. Thus, a better performance of RCS reduction than the absorber can be obtained by ACM. In other words, because of the low ratio of '0' elements, better RCS reduction can be achieved by removing the little '1' elements from an entire metamaterial absorber (in this paper, $M = N = 8, \alpha = 3/61$).

To verify via experiment the performance of the optimal ACM, a sample and a PEC grounded planar of equivalent geometry as a reference are fabricated and measured. Figure 8 illustrates the photograph view of the optimal ACM and the environment to make the measurement. The absorptive '1' element is made from carbon films prepared by spraying technique, and the surface resistance is controlled by the

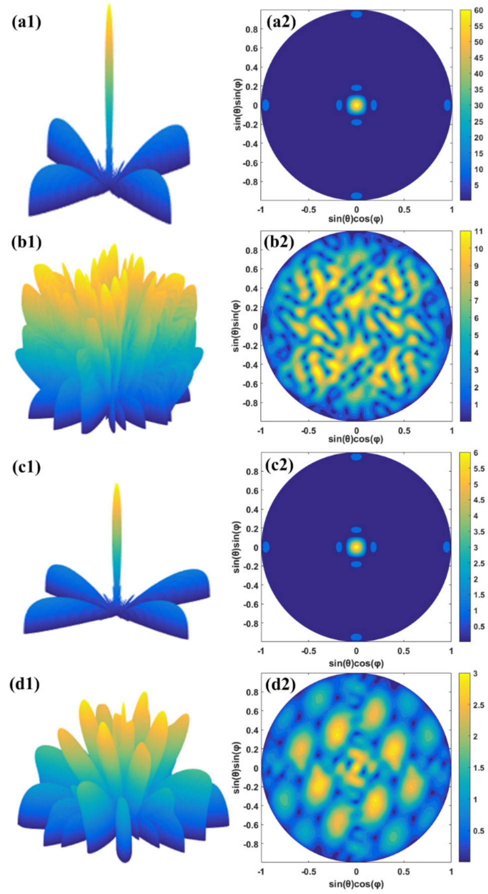

Figure 5. (1) and (2) demonstrate 3D and contour plot of formula-predicted scattering pattern, respectively. (a1) and (a2) demonstrate the pattern of PEC ground planar; (b1) and (b2) show optimal pattern with non-absorption coding sequence; (c1) and (c2) show the pattern of absorber with 90% absorption; (d1) and (d2) show the optimal pattern of 90% absorption of '1' element and non-absorption '0' element.

four-point probe. Both sizes of coding elements '0' and '1' are 22.5 mm (~λ) and the whole size of the fabricated sample is 180×180 mm, because the far-field certification of $R > 2D^2/\lambda_{\min}$. The scattering performance is evaluated by the transmission coefficients obtained by vector network analyzer Agilent N5230C. Figure 8(c) demonstrates the experimental results. The figure indicates that RCS reduction of over 10 dB is generated in the frequency range of 6.5–20 GHz, which generally has good agreement with the simulation results in the overall trends. The measurement error is mainly induced by the test environment of an incomplete anechoic chamber and the lossy material of metal.

For a better understanding of the role of element loss in total RCS reduction, we append an experimental result of RCS pattern cuts (in the $\varphi = 0^{\circ}$ and $\varphi = 90^{\circ}$ plane) pertaining to the ACM prototype, a metallic reference sample of the same size and a metamaterial absorber with an RFSS of the same size. As shown in figure 9, comparisons among ACM, metamaterial absorber with RFSS and metallic reference target with the same size are demonstrated. Both in the $\varphi = 0^{\circ}$ and $\varphi = 90^{\circ}$ planes, an RCS reduction of about 20 dB more than a metallic sample of same size and an RCS reduction of about 2 dB more than a metamaterial absorber with the same size is

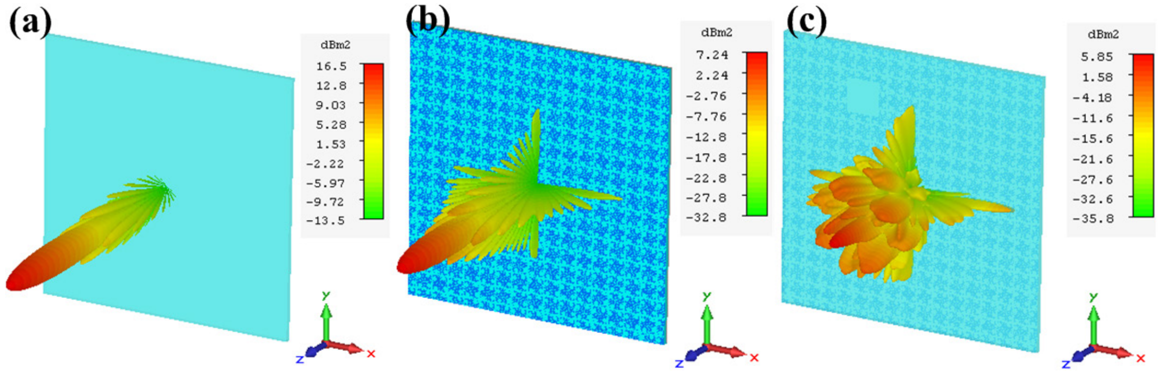

Figure 6. The full wave simulated 3D scattering pattern of (a) PEC ground planar, (b) absorber, (c) ACM, at 18 GHz.

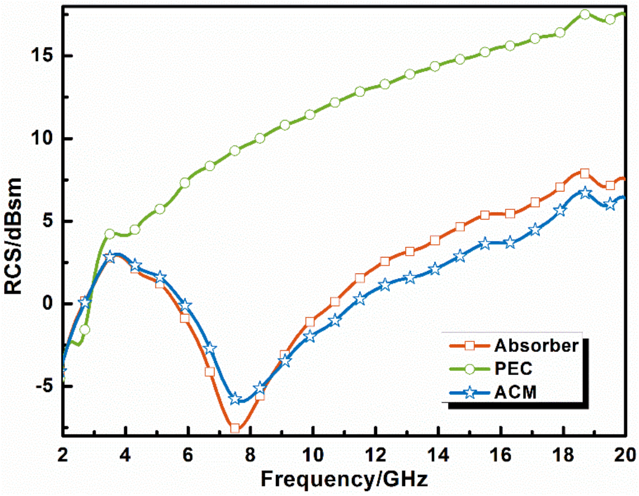

Figure 7. Simulated RCS of the PEC, absorber and optimal ACM in normal incidence.

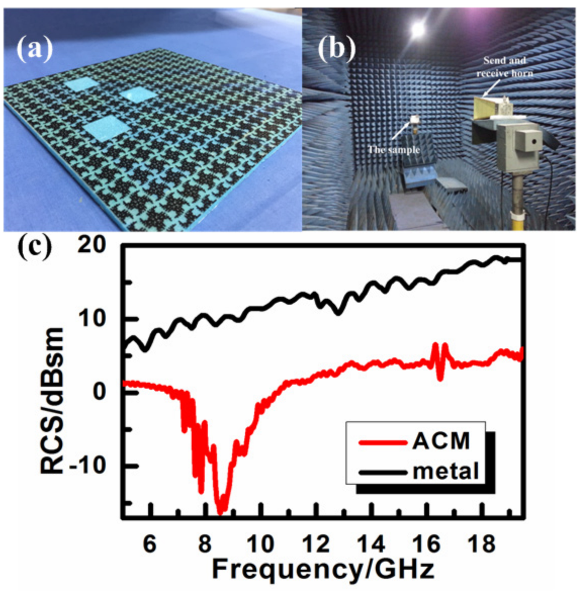

Figure 8. Photograph views of the fabricated sample (a) and (b) the environment of measurement. (c) The experiment results of RCS.

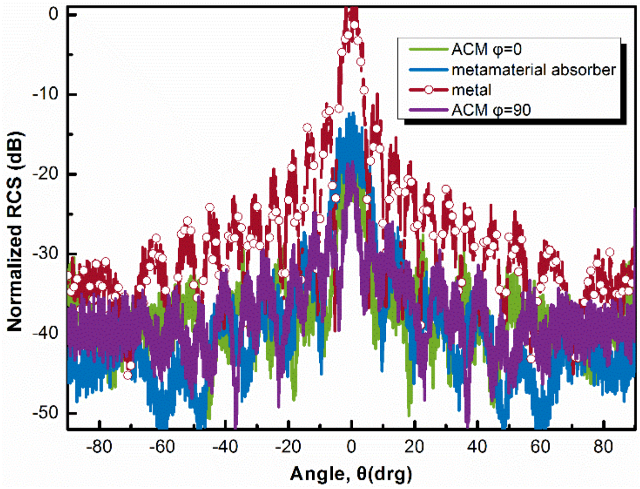

Figure 9. Measured results of normalized RCS cuts (in the $\varphi = 0$ and $\varphi = 90$ planes) pertaining to the ACM prototype, metamaterial absorber and metallic sample with same size.

experimentally observed. Besides, an extraordinary increase of RCS occurs in the range of $\theta \geqslant 25°$ compared with the metamaterial absorber, which means the remainder energy is re-distributed to oblique angles.

Conclusion

In summary, we proposed the ACM. The ACM is capable of shaping scattering patterns and, as an application, wideband bistatic RCS reduction of ACM is established. A new strategy combined with the metamaterial absorber and coding metasurface can mean that scattering energy can be both absorbed and redirected. A theoretical analysis of the influence of ratio and absorption efficiency is proposed. As a result, the ACM could achieve better RCS reduction performance than the metamaterial absorber or coding metasurface. According to the ACM theory, removing the little absorptive element could achieve better performance for RCS reduction. This idea of symmetry breaking, combining with ACM, is exciting for metamaterial absorber design and maintenance, which provides a new opportunity for stealth technology.

Acknowledgments

The authors are grateful to the support from the National Natural Science Foundation of China (Grants Nos. 61331005, 61671467, 61501497), the Innovation Team of Shaanxi province (Grant No. 2014KCT-05).

ORCID iDs

Sai Sui https://orcid.org/0000-0002-8160-1689
Hua Ma https://orcid.org/0000-0002-3560-7991

References

[1] Cui T J, Smith D and Liu R 2009 *Metamaterials: Theory, Design, and Applications* (Berlin: Springer) (https://doi.org/10.1007/978-1-4419-0573-4)
[2] Pendry J B, Schurig D and Smith D R 2006 Controlling electromagnetic fields *Science* **312** 1780
[3] Smith D R, Pendry J B and Wiltshire M C 2004 Metamaterials and negative refractive index *Science* **305** 788
[4] Yu N *et al* 2011 Light propagation with phase discontinuities reflection and refraction *Science* **334** 333
[5] Landy N I, Sajuyigbe S, Mock J J, Smith D R and Padilla W J 2008 Perfect metamaterial absorber *Phys. Rev. Lett.* **100** 207402
[6] Sun L K, Cheng H F, Zhou Y J and Wang J 2012 Broadband metamaterial absorber based on coupling resistive frequency selective surface *Opt. Express* **20** 4675
[7] Narimanov E E and Kildishev A V 2009 Optical black hole: broadband omnidirectional light absorber *Appl. Phys. Lett.* **95** 041106
[8] Cheng Q, Cui T J, Jiang W X and Cai B G 2010 An omnidirectional electromagnetic absorber made of metamaterials *New J. Phys.* **12** 063006
[9] Cui Y X, He Y R, Jin Y, Ding F, Yang L, Ye Y Q, Zhong S M, Lin Y Y and He S L 2014 Plasmonic and metamaterial structures as electromagnetic absorbers *Laser Photonics Rev.* **8** 495–520
[10] Liu Y H and Zhao X P 2014 Perfect absorber metamaterial for designing low-RCS patch antenna *IEEE Antennas Wirel. Propag. Lett.* **13** 1473–6
[11] Liu Y H, Gu S, Luo C R and Zhao X P 2012 Ultra-thin broadband metamaterial absorber *Appl. Phys.* A **18** 19–24
[12] Paquay M, Iriarte J C, Ederra I, Gonzalo R and Maagt P D 2007 Thin amc structure for radar cross-section reduction *IEEE Trans. Antennas Propag.* **55** 3630–8
[13] Hou Y C, Liao W J, Tsai C C and Chen S H 2016 Planar multilayer structure for broadband broad-angle rcs reduction *IEEE Trans. Antennas Propag.* **64** 1859–67
[14] Edalati A and Sarabandi K 2014 Wideband, wide angle, polarization independent rcs reduction using nonabsorptive miniaturized-element frequency selective surfaces *IEEE Trans. Antennas Propag.* **62** 747–54
[15] Cui T J, Qi M Q, Wan X, Zhao J and Cheng Q 2014 Coding metamaterials, digital metamaterials and programmable metamaterials *Light Sci. Appl.* **3** e218
[16] Gao L H *et al* 2015 Broadband diffusion of terahertz waves by multi-bit coding metasurfaces *Light Sci. Appl.* **4** e324
[17] Liu S and Cui T J 2017 Flexible controls of terahertz waves using coding and programmable metasurfaces *IEEE J. Sel. Top. Quantum Electron.* **23** 1–12
[18] Cui T J, Liu S and Li L L 2016 Information entropy of coding metasurface *Light Sci. Appl.* **5** e16172
[19] Ke W, Jie Z, Qiang C, Di S D and Cui T J 2014 Broadband and broad-angle low-scattering metasurface based on hybrid optimization algorithm *Sci. Rep.* **4** 5935
[20] Yan X *et al* 2015 Broadband, wide-angle, low-scattering terahertz wave by a flexible 2-bit coding metasurface *Opt. Express* **23** 29128
[21] Balanis C A 2005 *Antenna Theory: Analysis and Design* 3rd edn (New York: Wiley)
[22] Sui S, Ma H, Wang J, Pang Y and Qu S 2015 Topology optimization design of a lightweight ultra-broadband wide-angle resistance frequency selective surface absorber *J. Phys. D: Appl. Phys.* **48** 215101